MODERATELY LARGE DEFLECTION ANALYSIS OF SANDWICH ELLIPTICAL ARCS VIA MIXED FINITE ELEMENT METHOD

Elif Koc[1], Emre Kahraman[1], Umit N. Aribas[1], Merve Ermis[2], and Mehmet H. Omurtag[1]

[1]Istanbul Medipol University, School of Engineering and Natural Sciences, Department of Civil Engineering, 34810, Istanbul, Türkiye

[2]Kirklareli University, Faculty of Engineering, Department of Civil Engineering, 39000, Kirklareli, Türkiye

ABSTRACT

This study examines the moderately large deflections of sandwich elliptical arcs subjected to the in-plane loadings using the mixed finite element method. The constitutive equations, satisfying the classical beam stress-free surface conditions, are derived based on von Kármán nonlinear strains. The nonlinear equations of the mixed finite element formulation are derived based on the first variation of the Hellinger-Reissner functional, incorporating field equations and boundary conditions. Each node of the two-noded mixed finite elements has twelve degrees of freedom. The moderately large deflections of sandwich elliptical arcs, obtained via the mixed finite element method, are compared with the four-noded SHELL181 elements of ANSYS. Additionally, the effects of stiffener thickness and lamination are investigated in the scope of the parametric analyses.

Keywords: Moderately large deflection; Elliptical arcs; Sandwich beams; Transversely-isotropic materials; mixed finite element

INTRODUCTION

Laminated composite structures are widely employed in modern engineering due to their superior strength-to-weight ratio, tunable mechanical properties, and adaptability for complex load conditions. These structures, consisting of multiple fiber-reinforced layers, exhibit anisotropic behavior, enabling tailored designs for aerospace, automotive, and marine applications [1]. Among laminated composites, sandwich structures offer further advantages by combining stiff, high-strength outer skins with a lightweight core, enhancing structural efficiency, impact resistance, and buckling resistance [2]. While traditional straight beams have been extensively studied, curved laminated composite beams are critical in applications requiring enhanced load-bearing capacity and geometric adaptability, such as aerospace frames, biomedical implants, and bridge structures. The inherent curvature introduces additional stress components, leading to more complex mechanical behavior than straight beams. Nonlinear effects become prominent in curved composite structures, particularly at higher loads, where geometric nonlinearities significantly influence their response [3].

Several studies have examined the geometrically nonlinear behavior of curved beams/panels or sandwich structures. Bozhevolnaya and Frostig [4] developed a high-order analytical theory for

sandwich panels, incorporating transverse flexibility, shear rigidity, and geometric nonlinearity, extending their formulation to sandwich panels with constant curvature. Frostig and Thomsen [5] further analyzed the nonlinear response of sandwich panels with compliant cores, considering thermomechanical loading effects and high-order deformation mechanisms. Duan et al. [6] formulated a finite element (FE) model for nonlinear free vibration of thin-walled curved beams, integrating flexural–torsional coupling and warping effects. Yau and Yang [7] introduced a structural approach for bending-tension coupling in curved beams by developing an explicit elastic stiffness matrix, providing an alternative to conventional FE techniques. Other numerical methods have been explored to analyze nonlinear behavior in curved beams. Kurtaran [8] applied the generalized differential quadrature method (GDQM) for the geometrically nonlinear transient analysis of deep laminated curved beams, incorporating Green–Lagrange strain-displacement relations and first order shear deformation theory. Liao et al. [9] developed a quadrature element method (QEM) for curved beams, capturing large three-dimensional rotations and postbuckling behavior. Li et al. [10] investigated functionally graded (FG) curved sandwich beams with a self-adapted auxetic 3D meta-lattice core, analyzing graphene-reinforced composite facesheets under nonlinear dynamic conditions. Nasri et al. [11] analyzed the buckling and nonlinear bending response of 3D-printed polymeric meta-sandwich curved beams using first-order shear deformation theory and von-Kármán nonlinearity to derive the nonlinear governing equations for beams under uniform transverse and axial loads. Their results, validated via the Ritz method, assessed the influence of various geometrical parameters on buckling resistance and bending response, optimizing these parameters to enhance buckling resistance and minimize transverse deflection. Serveren et al. [12] conducted a geometrically nonlinear dynamic analysis of three-layered curved sandwich beams with a viscoelastic core, employing Hamilton's principle and GDQM to examine resonance and nonlinear vibration effects. Wen and Li [13] analyzed the lateral-torsional buckling (LTB) behavior of curved beams, identifying neglected end moments and redundant distributed moments, leading to a refined FE model for elastic LTB analysis.

Despite these advancements, the moderately large deflection analysis of sandwich elliptical arcs remains an open research area, as existing studies have primarily focused on straight beams, thin-walled curved beams, or planar sandwich panels. In this study, a mixed finite element method is developed for the moderately large deflections of sandwich elliptical arcs, incorporating von Kármán nonlinear strains. The nonlinear field equations are derived from the first variation of the Hellinger-Reissner functional, ensuring a robust mathematical framework. The two-noded mixed finite elements, each possessing twelve degrees of freedom, enable an accurate representation of the nonlinear structural response. To validate the proposed method, results are compared with four-noded SHELL181 element simulations, ensuring accuracy in predicting moderately large deflections. Furthermore, the influence of stiffener thickness and lamination configurations on structural behavior is examined. By integrating a mixed finite element formulation with nonlinear elasticity theory, this study provides a comprehensive computational framework for analyzing curved sandwich beams, offering valuable insights into their behavior under large deformations.

FIELD EQUATIONS and FORMULATION

The constitutive equations relating the three-dimensional stress vector $\boldsymbol{\sigma}$ and strain vector $\boldsymbol{\varepsilon}$ over the elasticity matrix $\mathbf{E}$ are defined based on the Hooke's law as $\boldsymbol{\sigma} = \mathbf{E}\boldsymbol{\varepsilon}$ [14]. The classical beam stress-free surface conditions are satisfied on the constitutive equations and given in [15] as $\boldsymbol{\sigma}_L = \boldsymbol{\beta}_L \boldsymbol{\varepsilon}_L$ where, the subscript L presents the layer partition, $\boldsymbol{\beta}_L$ is a 3×3

matrix, $\boldsymbol{\sigma}_L = \{\sigma_t \quad \tau_{bt} \quad \tau_{tn}\}_L^{\mathrm{T}}$ and $\boldsymbol{\varepsilon}_L = \{\varepsilon_t \quad \gamma_{bt} \quad \gamma_{tn}\}_L^{\mathrm{T}}$. Letting t,n,b are the Frenet Coordinates, the displacement field of the sandwich beam is given as,

$$u_t^* = u_t + b\,\Omega_n - n\,\Omega_b \quad ; \quad u_n^* = u_n - b\,\Omega_t \quad ; \quad u_b^* = u_b + n\,\Omega_t \tag{1}$$

where, the displacements on the beam axis are u_t, u_n, u_b, and the rotations are $\Omega_t, \Omega_n, \Omega_b$. Von Kármán nonlinear strains are derived by means of the displacement field as,

$$\begin{aligned}
\varepsilon_t^* &= u_{t,t}^* + \tfrac{1}{2}\left[\left(u_{t,t}^*\right)^2 + \left(u_{n,t}^*\right)^2 + \left(u_{b,t}^*\right)^2\right] \\
\varepsilon_{tn}^* &= \tfrac{1}{2}\left[u_{t,n}^* + u_{n,t}^* + u_{t,t}^*\,u_{t,n}^* + u_{n,t}^*u_{n,n}^* + u_{b,t}^*u_{b,n}^*\right] \\
\varepsilon_{bt}^* &= \tfrac{1}{2}\left[u_{t,b}^* + u_{b,t}^* + u_{t,t}^*\,u_{t,b}^* + u_{n,t}^*\,u_{n,b}^* + u_{b,t}^*u_{b,b}^*\right]
\end{aligned} \tag{2}$$

where, the commas in the subscripts denote the partial derivations. The forces F_t, F_n, F_b and the moments M_t, M_n, M_b can be obtained by the integration of stresses based on Von Kármán nonlinear strains through the thickness [16]. Finally, the explicit form of the equilibrium equations are as follows:

$$\begin{aligned}
&-F_{t,s} - \left(F_t\,u_{t,s}\right)_{,s} - \left(M_n\Omega_{n,s}\right)_{,s} - \left(M_b\Omega_{b,s}\right)_{,s} + \left(F_n\Omega_b\right)_{,s} - \left(F_b\Omega_n\right)_{,s} - q_t = 0 \\
&-F_{n,s} - \left(F_t\,u_{n,s}\right)_{,s} + \left(M_n\Omega_{t,s}\right)_{,s} + \left(F_b\Omega_t\right)_{,s} - q_n = 0 \\
&-F_{b,s} - \left(F_t\,u_{b,s}\right)_{,s} + \left(M_b\Omega_{t,s}\right)_{,s} - \left(F_n\Omega_t\right)_{,s} - q_b = 0 \\
&-M_{t,s} + \left(M_n u_{n,s}\right)_{,s} + \left(M_b u_{b,s}\right)_{,s} + F_n u_{b,s} - F_b u_{n,s} - M_{t,s} - m_t = 0 \\
&-M_{n,s} + F_b - \left(M_n u_{t,s}\right)_{,s} - \left(M_t\Omega_b\right)_{,s} + F_b u_{t,s} - M_t\Omega_{b,s} - m_n = 0 \\
&-M_{b,s} - F_n - \left(M_b u_{t,s}\right)_{,s} - F_n u_{t,s} + M_t\Omega_{n,s} + \left(M_t\Omega_n\right)_{,s} - m_b = 0
\end{aligned} \tag{3}$$

where, q_t, q_n, q_b are the external distributed forces, m_t, m_n, m_b are the external distributed moments, and s is the axial arc length. The position vector $\mathbf{r}\ \theta$ in terms of the horizontal angle θ, and the gradient of the arc length $c\ \theta$ of exact elliptical beams is given in Ermis et al. [17]. The first variation of Hellinger Reissner functional [18] is obtained from the field equations and boundary conditions such as,

$$\delta\Pi_{HR} = \int_V \left(\boldsymbol{\varepsilon}^{\mathrm{u}} - \boldsymbol{\varepsilon}^{\sigma}\right)^T \delta\boldsymbol{\sigma}^{\sigma}\,\mathrm{d}V + \int_V \left(\left(\boldsymbol{\sigma}^{\sigma}\right)^T \delta\boldsymbol{\varepsilon}^{\mathrm{u}} - \mathbf{q}^T\delta\mathbf{u}\right)\mathrm{d}V - \int_\Gamma \hat{\mathbf{t}}^T\delta\mathbf{u}\,\mathrm{d}\Gamma = 0 \tag{4}$$

where, $\hat{\mathbf{t}}$ is the traction vector at the boundary Γ, and the superscripts σ and u denote the components defined in terms of the forces and displacements. In the scope of the field equations, the variational equations in the mixed form are obtained,

$$\int_S \begin{pmatrix} \left[u_{t,s} + \tfrac{1}{2}u_{t,s}^2 + \tfrac{1}{2}u_{n,s}^2 + \tfrac{1}{2}u_{b,s}^2 - C_{11}F_t - C_{12}F_n - C_{14}M_t - C_{15}M_n\right]\delta F_t \\ +\left[u_{n,s} - \Omega_b - u_{t,s}\Omega_b + u_{b,s}\Omega_t - C_{12}F_t - C_{22}F_n - C_{24}M_t - C_{25}M_n\right]\delta F_n \\ +\left[u_{b,s} + \Omega_n + u_{t,s}\Omega_n - u_{n,s}\Omega_t - C_{33}F_b\right]\delta F_b \\ +\left[\Omega_{t,s} + \Omega_{n,s}\Omega_b - C_{14}F_t - C_{24}F_n - C_{44}M_t - C_{45}M_n\right]\delta M_t \\ +\left[\Omega_{n,s} + u_{t,s}\Omega_{n,s} - u_{n,s}\Omega_{t,s} - C_{15}F_t - C_{25}F_n - C_{45}M_t - C_{55}M_n\right]\delta M_n \\ +\left[\Omega_{b,s} + u_{t,s}\Omega_{b,s} - u_{b,s}\Omega_{t,s} - C_{66}M_b\right]\delta M_b - \delta u_t q_t - \delta u_n q_n - \delta u_b q_b \\ -\delta\Omega_t m_t - \delta\Omega_n m_n - \delta\Omega_b m_b + \left[T_t + T_t u_{t,s} + M_n\Omega_{n,s} + M_b\Omega_{b,s} - T_n\Omega_b + T_b\Omega_n\right]\delta u_{t,s} \\ +\left[T_n + T_t u_{n,s} - M_n\Omega_{t,s} - T_b\Omega_t\right]\delta u_{n,s} + \left[T_b + T_t u_{b,s} - M_b\Omega_{t,s} + T_n\Omega_t\right]\delta u_{b,s} \\ +\left[T_n u_{b,s} - T_b u_{n,s}\right]\delta\Omega_t + \left[M_t - M_n u_{n,s} - M_b u_{b,s}\right]\delta\Omega_{t,s} + \left[T_b + T_b u_{t,s}\right]\delta\Omega_n \\ +\left[M_n + M_n u_{t,s} + M_t\Omega_b\right]\delta\Omega_{n,s} + \left[-T_n - T_n u_{t,s} + M_t\Omega_{n,s}\right]\delta\Omega_b + \left[M_b + M_b u_{t,s}\right]\delta\Omega_{b,s} \end{pmatrix} \mathrm{d}s \quad (5)$$

By linearizing the nonlinear equations [19,20], the functional is obtained and the iterative solution approach is performed based on the Newton-Raphson algorithm [18].

NUMERICAL EXAMPLES

In this section, first, the finite element (FE) mesh convergence analyses are performed for the moderately large displacements of a sandwich elliptical arc via both the two-noded mixed FEs and four-noded SHELL181 elements of ANSYS. The convergence performance of these elements is evaluated based on the degrees of freedom (DOFs) they use, and the converged results of both elements are compared. Next, the influence of cross-sectional dimensions on the difference between the geometrically nonlinear and linear displacements is studied via parametric analyses. In all convergence and parametric analyses, the opening angle is $\varphi = 90°$. The maximum and minimum radii of the sandwich elliptical arc are $R_{\max} = 2\mathrm{m}$ and $R_{\min} = 1.6\mathrm{m}$, respectively. The end with a radius of 2 meters is fixed, and at the other end, all displacement and rotation degrees of freedom are fixed except the in-plane displacement (Figure 1). The width of the cross-section is $w = 0.25\mathrm{m}$. Both stiffeners of the sandwich cross-section have equal thickness. The core is made of Kevlar 49-Epoxy and the stiffeners are Boron Epoxy. The Young's moduli, shear moduli and Poisson's ratios of Boron Epoxy are $E_t = 241.5\,\mathrm{GPa}$, $E_n = E_b = 18.89\,\mathrm{GPa}$, $G_{tn} = G_{bt} = 5.18\,\mathrm{GPa}$, $G_{nb} = 3.45\,\mathrm{GPa}$, $\upsilon_{tn} = \upsilon_{tb} = 0.24$ and $\upsilon_{nb} = 0.25$, respectively. The Young's moduli, shear moduli and Poisson's ratios of Kevlar 49-Epoxy are $E_t = 76\,\mathrm{GPa}$, $E_n = E_b = 5.56\,\mathrm{GPa}$, $G_{tn} = G_{bt} = 2.30\,\mathrm{GPa}$, $G_{nb} = 1.618\,\mathrm{GPa}$, $\upsilon_{tn} = \upsilon_{tb} = 0.34$, $\upsilon_{nb} = 0.718$, respectively. The sandwich elliptical arc is subjected to a uniform pressure perpendicular to its' inner surface.

FE Mesh Convergence Analyses

SHELL181 Elements: The moderately large displacements $u_{b\ \mathrm{nl}}$ at the vertical guided fixed support of a sandwich elliptical arc (Figure 1) are obtained using 18000, 42000, 93648, 273324 and 882504 DOFs, respectively (successively corresponding to 0.05m, 0.02m, 0.01m, 0.005m and 0.0025m mesh sizes). The thickness of each stiffener is $h_s = 0.0025\mathrm{m}$ and the total cross-sectional thickness is $h = 0.03\mathrm{m}$. The uniform pressure acting perpendicular to the inner surface is $q_b = 2.64\mathrm{bar}$. The results are tabulated in Table 1 compared to the displacements of

linear analysis $u_{b\ l}$. It is obtained that the percent difference in $u_{b\ nl}$, with respect to the results obtained using 882504 DOFs, decreases below 1.00% in the analysis performed with 273324 DOFs. Besides, the percent difference between geometrically nonlinear and linear displacements is obtained as -29.93% relative to the results of linear analysis.

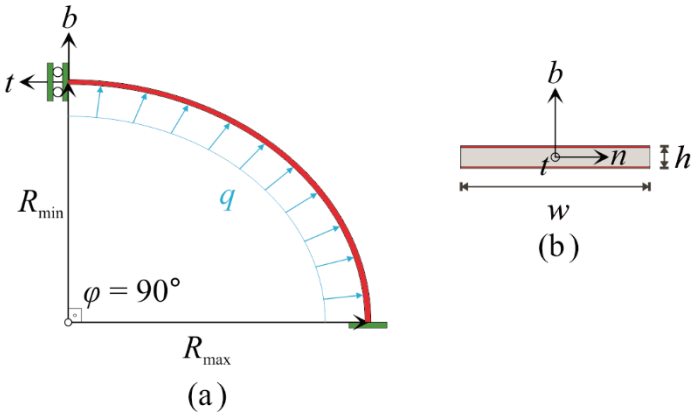

Figure 1. (a) Elliptical arc subjected to a uniform pressure, (b) The sandwich cross-section.

Table 1. FE mesh convergence of the displacements (in meters) for SHELL181 elements.

DOFs	$u_{b\ l}$	$u_{b\ nl}$	diff.[1]%	diff.[2]%
18000	0.035764	0.024467	15.49	-31.59
42000	0.035679	0.024622	16.22	-30.99
93648	0.030957	0.021711	2.48	-29.87
273324	0.030465	0.021346	0.76	-29.93
882504	0.030233	0.021185		-29.93

*Note: the percent difference of moderately large displacements (diff.[1]%) is given relative to 882504 DOFs, and the percent difference of geometrically nonlinear and linear displacements (diff.[2]%) is given relative to the linear results.

Table 2. FE mesh convergence of the displacements (in meters) for the mixed FEs.

DOFs	$u_{b\ l}$	$u_{b\ nl}$	diff.[1]%	diff.[2]%
132	0.030909	0.021219	0.30	-31.35
192	0.029646	0.020915	-1.14	-29.45
312	0.029877	0.021113	-0.21	-29.33
612	0.030037	0.021155	-0.01	-29.57
1212	0.030000	0.021156	0.00	-29.48
1812	0.029993	0.021156	0.00	-29.46
2412	0.029991	0.021156	0.00	-29.46
3012	0.029990	0.021156		-29.46

*Note: the percent difference of moderately large displacements (diff.[1]%) is given relative to 3012 DOFs, and the percent difference of geometrically nonlinear and linear displacements (diff.[2]%) is given relative to the linear results.

Mixed FEs: The FE mesh convergence analysis of the above-mentioned problem is performed using 132-3012 DOFs, respectively (Table 2). It is obtained that the percent difference in $u_{b\ nl}$, with respect to the results obtained using 3012 DOFs, decreases below 1.00% in the analysis performed with 312 DOFs. The geometrically nonlinear mixed FE formulation provides quite satisfactory results using fewer degrees of freedom compared to the four-node SHELL181 elements of ANSYS. The percent differences of linear and geometrically nonlinear

displacements obtained by the mixed FEs with 3012 DOFs relative to the SHELL181 elements with 882504 DOFs are -0.80% and -0.14%, respectively. Besides, the percent difference between geometrically nonlinear and linear displacements is obtained as -29.33% relative to the results of linear analysis.

The thicknesses of stiffeners and cross-section

This section aims to investigate the influence of thicknesses of stiffeners and the cross-section on the percent difference between the linear and geometrically nonlinear displacements of sandwich elliptical arcs. Thus, the total cross-sectional thickness is set to $h = 0.020\text{m}$, 0.025m and 0.030m, respectively. In each case, the thickness of stiffeners is set to $h_s = 0.0015\text{m}$, 0.002m and 0.0025m, respectively by keeping the total cross-sectional thickness constant. The corresponding geometrically nonlinear displacements $u_{b\ \text{nl}}$, under the same magnitude of pressure that the linear displacements are obtained, are illustrated in Figure 2. Then, the percent differences of geometrically nonlinear displacements $u_{b\ \text{nl}}$ with respect to the linear displacements $u_{b\ 1}$ are given in Figure 3.

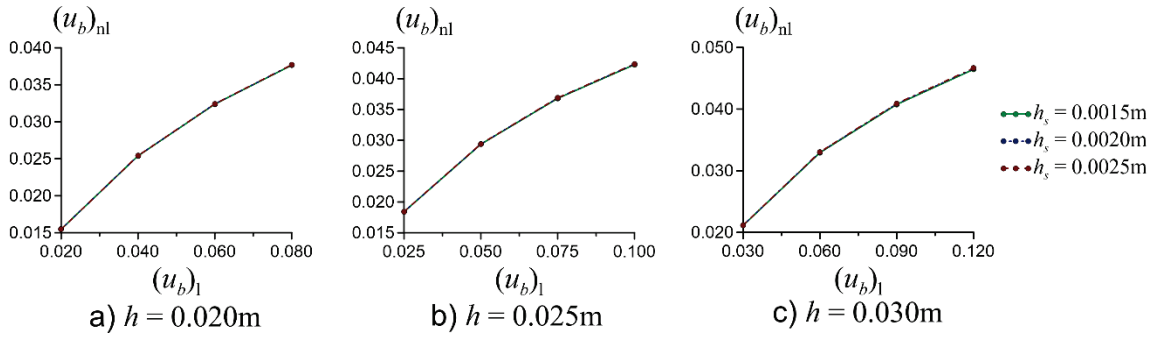

Figure 2. The geometrically nonlinear and linear displacements.

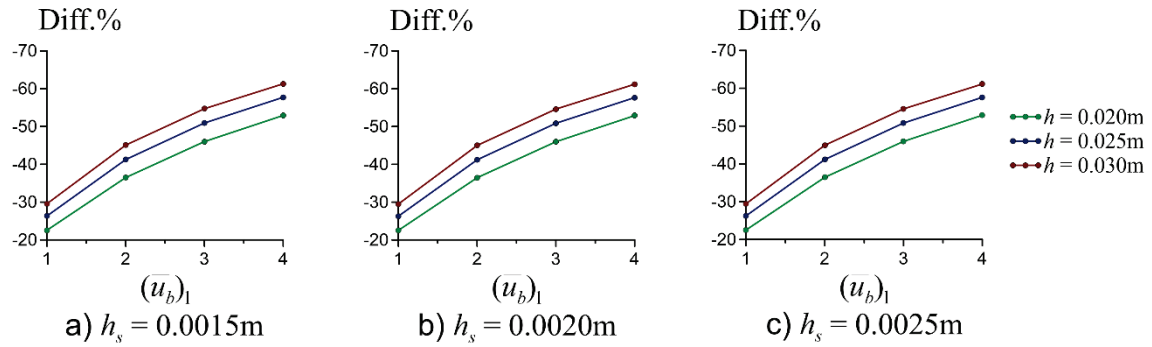

Figure 3. The percent difference of geometrically nonlinear displacements $u_{b\ \text{nl}}$ with respect to the linear displacements $u_{b\ 1}$. $\overline{u}_{b\ 1} = u_{b\ 1}/h$: The normalized linear displacements.

It is concluded that a decrease in stiffener thickness and/or an increase in cross-sectional thickness results in an increase in the percent difference between geometrically nonlinear and linear displacements. The influence of an increase in cross-sectional thickness is greater than the stiffener thickness. Although the linear displacement occurs at the section height, the minimum absolute percentage difference of the corresponding geometrically nonlinear displacement with respect the linear displacement is obtained as 22.54% in the case of $h = 0.020\text{m}$ and $h_s = 0.0025\text{m}$. As the stiffener thickness decreases to $h_s = 0.0015\text{m}$ in this case, this absolute percent difference increases to 22.57%. However, when the linear

displacement reaches four times the section height, this absolute percent difference increases up to 52.94%. In cases where the linear displacement value is smaller, the percentage increases in the percent differences are greater. As the cross-sectional thickness increases up to $h = 0.030\text{m}$ and the stiffener thickness decreases to $h_s = 0.0015\text{m}$, the absolute percent difference between the geometrically nonlinear and linear displacements increases up to 61.30% when the linear displacement reaches four times the section height.

CONCLUSIONS

This study focuses on analyzing moderately large deflections in sandwich elliptical arcs subjected to in-plane loading, utilizing a mixed finite element method. The constitutive relations are formulated based on von Kármán-type geometric nonlinearity and the classical beam stress-free surface conditions. The mixed finite element formulation is developed by taking the first variation of the Hellinger-Reissner functional. Each two-noded mixed finite element has twelve degrees of freedom at per node. The deflection results obtained from the proposed mixed finite element approach are compared with the four-noded SHELL181 elements. The geometrically nonlinear mixed finite elements provide convergent results with fewer degrees of freedom compared to the four-node SHELL181 elements of ANSYS. As a conclusion of the parametric analysis, it is obtained that the influence of the cross-sectional thickness on the percent difference between geometrically nonlinear and linear displacements is greater than the stiffener thickness. Although the linear displacement occurs at the section height for the minimum cross-sectional thickness and maximum stiffener thickness, the minimum percent difference is obtained as -22.54%.

REFERENCES

[1] C. Hwu, Mechanics of Laminated Composite Structures, CRC Press, 2024.

[2] S.H. Sandeep, C.V. Srinivasa, Hybrid sandwich panels: a review, International Journal of Applied Mechanics and Engineering 25 (2020) 64–85.

[3] G.A. Drosopoulos, G.E. Stavroulakis, Nonlinear Mechanics for Composite Heterogeneous Structures, CRC Press, Boca Raton, 2022. https://doi.org/10.1201/9781003017240.

[4] E. Bozhevolnaya, Y. Frostig, Nonlinear closed-form high-order analysis of curved sandwich panels, Composite Structures 38 (1997) 383–394. https://doi.org/10.1016/S0263-8223(97)00073-1.

[5] Y. Frostig, O. Thomsen, Nonlinear behavior of thermally loaded curved sandwich panels with a transvesely flexible core, Journal of Mechanics of Materials and Structures 4 (2009) 1287–1326.

[6] H. Duan, Nonlinear free vibration analysis of asymmetric thin-walled circularly curved beams with open cross section, Thin-Walled Structures 46 (2008) 1107–1112. https://doi.org/10.1016/j.tws.2008.01.002.

[7] J.D. Yau, Y.B. Yang, Geometrically nonlinear analysis of planar circular arches based on rigid element concept — A structural approach, Engineering Structures 30 (2008) 955–964. https://doi.org/10.1016/j.engstruct.2007.06.003.

[8] H. Kurtaran, Geometrically nonlinear transient analysis of thick deep composite curved beams with generalized differential quadrature method, Composite Structures 128 (2015) 241–250. https://doi.org/10.1016/j.compstruct.2015.03.060.